JOURNAL OF SYNCHROTRON RADIATION

ISSN 1600-5775

Received 11 May 2020
Accepted 26 August 2020

Edited by G. Grübel, HASYLAB at DESY, Germany

Keywords: X-ray free-electron lasers; two-color X-ray beams; self-seeding.

Two-color X-ray free-electron laser consisting of broadband and narrowband beams

Ichiro Inoue,[a]* Taito Osaka,[a] Toru Hara[a] and Makina Yabashi[a,b]

[a]XFEL Research and Development Division, RIKEN SPring-8 Center, 1-1-1 Kouto, Sayo, Hyogo 679-5148, Japan, and [b]Japan Synchrotron Radiation Research Institute, 1-1-1 Kouto, Sayo, Hyogo 679-5198, Japan.
*Correspondence e-mail: inoue@spring8.or.jp

A simple scheme is proposed and experimentally confirmed to generate X-ray free-electron lasers (XFELs) consisting of broadband and narrowband beams with a controllable intensity ratio and a large photon-energy separation. This unique two-color XFEL beam will open new opportunities for investigation of nonlinear interactions between intense X-rays and matter.

1. Introduction

Understanding interactions between intense light and matter is an intriguing subject from the viewpoints of basic sciences and practical applications. The advent of X-ray free-electron lasers (XFELs) (Emma *et al.*, 2010; Ishikawa *et al.*, 2012; Kang *et al.*, 2017; Decking *et al.*, 2020; Milne *et al.*, 2017), which generate brilliant X-ray pulses with femtosecond durations, extended this research field into the hard X-ray region. Soon after XFELs were realized, second-order non-linear X-ray optical phenomena, such as sum-frequency generation (Glover *et al.*, 2012) and second harmonic generation (Shwartz *et al.*, 2014), had been reported. Recently, higher-order X-ray optical phenomena became accessible (Tamasaku *et al.*, 2014, 2018; Ghimire *et al.*, 2016) by combining XFELs and up-to-date X-ray focusing optics (Mimura *et al.*, 2014).

Although a single X-ray beam has been utilized for these experiments, the use of multiple XFEL beams with flexible photon-energy separation drastically enhances the capability of XFELs. At beamline 3 (BL3) of SPring-8 Angstrom Compact free-electron LAser (SACLA) (Tono *et al.*, 2013; Yabashi *et al.*, 2015), a two-color XFEL beam can be generated by the split-undulator technique (Hara *et al.*, 2013). SACLA BL3 has twenty-one 5 m-long variable-gap undulators. In the split-undulator technique, all undulators are grouped into two sections and the gaps of the two sections are set at different deflection parameters. By independently amplifying the XFEL beams in the two sections through self-amplified spontaneous emission (SASE) (McNeil & Thompson, 2010) from a common electron bunch (e-bunch), SACLA can generate a two-color XFEL beam with a maximum photon-energy separation of 30% and a relative energy bandwidth ($\Delta E/E$) of ~0.3% for each color. The two-color XFEL beam has been utilized for various experiments, such as the time-resolved measurement of X-ray damage to matter (Inoue *et al.*, 2016), stimulated emission in the hard X-ray region (Yoneda *et al.*, 2015) and multi-wavelength anomalous diffraction phasing in serial femtosecond crystallography (Gorel *et al.*, 2017).

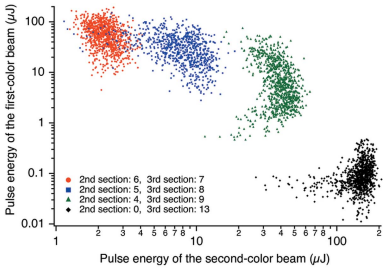

We here propose and demonstrate a new split-undulator scheme to generate a two-color XFEL consisting of narrowband ($\Delta E/E \sim 0.02\%$) and broadband ($\Delta E/E \sim 0.3\%$) beams. This unique XFEL beam will further expand the potential of XFELs for exploration and application of interactions between intense X-rays and matter. One of the potential applications is X-ray coherent anti-Stokes Raman scattering (XCARS) spectroscopy for low-Z elements such as carbon, sulfur and oxygen; the shape of the XCARS spectrum becomes the same as that of the K-edge absorption spectrum by using the narrowband beam as the pump light and the broadband beam as the Stokes light. Another possible application is creation and diagnostics of matter at high energy density, such as solid-density plasma (Vinko *et al.*, 2012), in which the broadband beam is used for exciting matter and the narrowband beam probes the excited states. Narrow bandwidth of the probe beam enables advanced diagnostic techniques, for example X-ray Thomson scattering (Glenzer & Redmer, 2009) and resonant inelastic X-ray scattering.

2. Concept

The schematic in Fig. 1 shows the concept for generating a two-color XFEL consisting of broadband and narrowband beams at SACLA. All undulators are grouped into three sections. Between the first and the second undulator sections, a pair of steering magnets, a magnetic chicane and a channel-cut X-ray crystal monochromator are installed.

The first-color beam with a narrow bandwidth is generated in the first and the second undulator sections via reflection-type self-seeding (Inoue *et al.*, 2019). The channel-cut crystal produces a seed beam by monochromatizing the SASE–XFEL beam from the first undulator section. Then, the seed beam is amplified in the second undulator section by setting the deflection parameter at the same value as that in the first undulator section. Here, for spatiotemporal overlap between the e-bunch and the seed beam in the second undulator section, the e-bunch is offset and detoured between the first and the second undulator sections using the steering magnets and the magnetic chicane. The third undulator section with a different deflection parameter produces the second-color beam with a broad bandwidth through SASE from the common e-bunch. The photon energies of the first-color and second-color beams are independently controllable by tuning the deflection parameters of the undulators. Furthermore, the pulse energy of each color can be adjusted by changing the undulator length of each section.

3. Experimental demonstration

To experimentally confirm the concept described above, a two-color XFEL consisting of 10 keV narrowband and 7.2 keV broadband beams was generated at SACLA BL3. The 7.8 GeV e-bunch with a charge of 130 pC and ~10 fs duration was injected into the undulators. The deflection parameter for each undulator section was set at 2.10 (the first and the second undulator sections) and 2.60 (the third undulator section) with a slight gap taper to compensate the energy loss of the e-bunch due to resistive wakefields. Eight upstream undulators were used as the first undulator section and generated a 10 keV SASE–XFEL beam. A silicon (Si) (220) channel-cut crystal with a gap of 97 μm (Osaka *et al.*, 2019), which was installed between the eighth and the ninth undulators, selected 10 keV radiation with an energy bandwidth of 0.6 eV in full width at half-maximum (FWHM) and an average pulse energy of 0.1 μJ. All existing undulators located downstream of the channel-cut crystal (thirteen undulators) were used for either amplifying the seed beam or generating the second-color beam with a central photon energy of 7.2 keV. The delay of the second-color beam with respect to the first-color beam, which was caused by the slippage effect in the third undulator section, was estimated to be less than 2 fs. As this value is

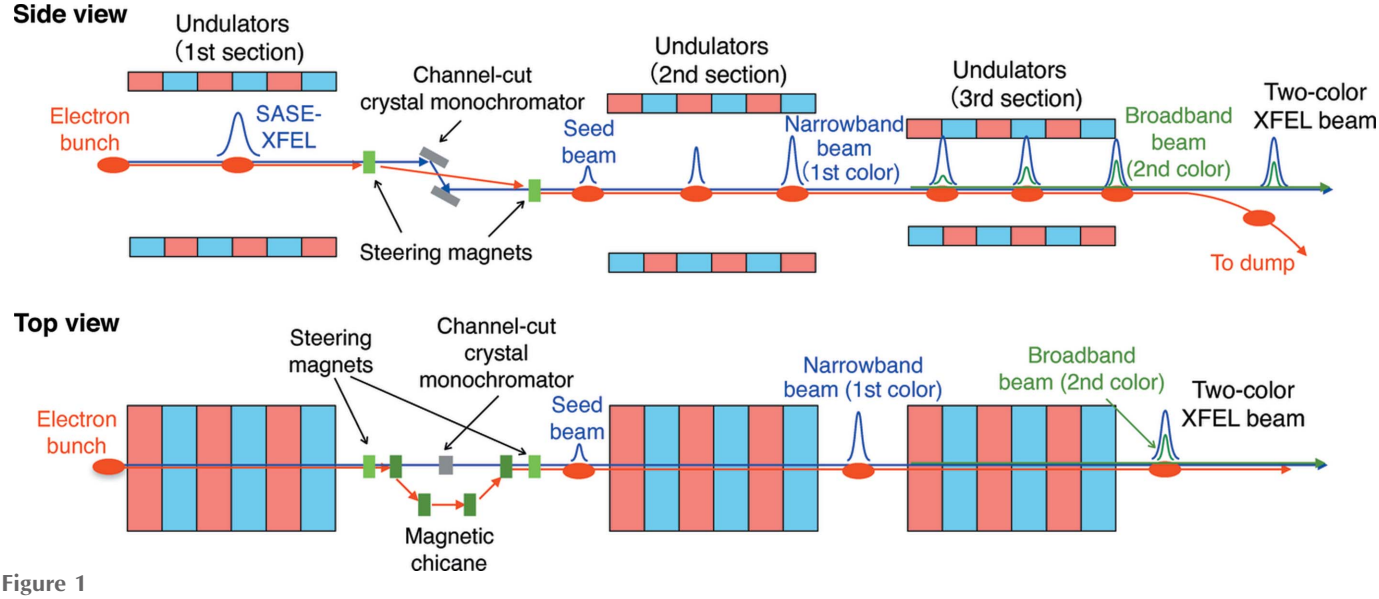

Figure 1
Schematic of a split-undulator scheme to generate a two-color XFEL consisting of narrowband and broadband beams at SACLA.

much shorter than the XFEL duration (6–8 fs in FWHM) (Inubushi *et al.*, 2017; Inoue *et al.*, 2018), the first-color and the second-color beams were almost temporally overlapped.

The spectrum of the two-color beam was measured by two dispersive spectrometers combined with a transmission grating beam splitter. The XFEL beam was multiplexed by the grating, and the transmitted beam and the primary diffracted beam were introduced to the spectrometers at experimental hutch 1 (EH1) and at experimental hutch 5 (EH5) (Tono *et al.*, 2013), respectively. Each spectrometer consisted of a focusing mirror for enlarging the divergence angle of the XFEL beam, a flat Si analyzer crystal [Si (111) crystal at EH1 and Si (331) crystal at EH4] and a multi-port charge-coupled device detector (Kameshima *et al.*, 2014). The spectrometer at EH1 (EH5) measured the spectrum of the second-color (the first-color) beam at a resolution of 1.1 eV (0.3 eV). Details about the grating, the spectrometer at EH1 and the focusing system at EH5 are described elsewhere (Katayama *et al.*, 2016; Yumoto *et al.*, 2020).

Fig. 2(*a*) shows average spectra of the two-color XFEL beam for different numbers of undulators in the second and the third sections. Except for the case when no undulator was used for amplifying the seed beam, $\Delta E/E$ of the first-color beam was ∼0.02% in FWHM, which was slightly larger than that of the seed beam. This broadening of the spectra can be explained by the presence of an energy chirp in the e-bunch (Inoue *et al.*, 2019). $\Delta E/E$ of the second-color beam was ∼0.3% in FWHM, which is comparable with that of normal SASE operation at SACLA. There was a negative correlation between the intensities of the first-color and the second-color beams, because the electron energy spread caused by the lasing of the first-color beam reduced the XFEL gain for the second-color (Xie, 2000).

This relation is more clearly shown in Fig. 2(*b*), in which shot-to-shot pulse energy correlation between the first-color and the second-color beams are plotted. Here the pulse energy of each color was measured using an inline spectrometer (Tono *et al.*, 2013) and a calibrated intensity monitor (Tono *et al.*, 2011). The intensity monitor evaluated the total pulse energy of the two-color XFEL beam, whereas the inline spectrometer monitored the pulse energy of the first-color or the second-color beam, whichever is weaker. By combining results of the measurements, the shot-to-shot pulse energy of each color was evaluated.

When six undulators were used to amplify the seed beam [red circles in Fig. 2(*b*)], lasing of the first-color beam was close to saturation and the average pulse energy of the first-color beam (60 µJ) was much larger than that of the second-color beam (2.3 µJ). As the undulator length in the third section became longer, the pulse energy of the second-color beam increased at the cost of a decrease in the pulse energy of the first-color beam. For each undulator condition shown in Fig. 2(*b*), the average pulse energy of the first-color beam was 60 µJ (red circles), 35 µJ (blue squares), 9.4 µJ (green triangles) and 0.1 µJ (black diamonds), whereas that of the second-color beam was 2.3 µJ (red circles), 8.1 µJ (blue squares), 39 µJ (green triangles) and 145 µJ (black diamonds). These results indicate that the intensity ratio between the first-color and the second-color beams is controllable over a wide range by changing the undulator length of each section. It is noteworthy that our method can generate an intense narrowband beam, compared with the case when the SASE–XFEL beam is simply monochromated; even if all undulators are employed for generating SASE beams at SACLA, the average pulse energy after an Si (220) channel-cut crystal is ∼8 µJ.

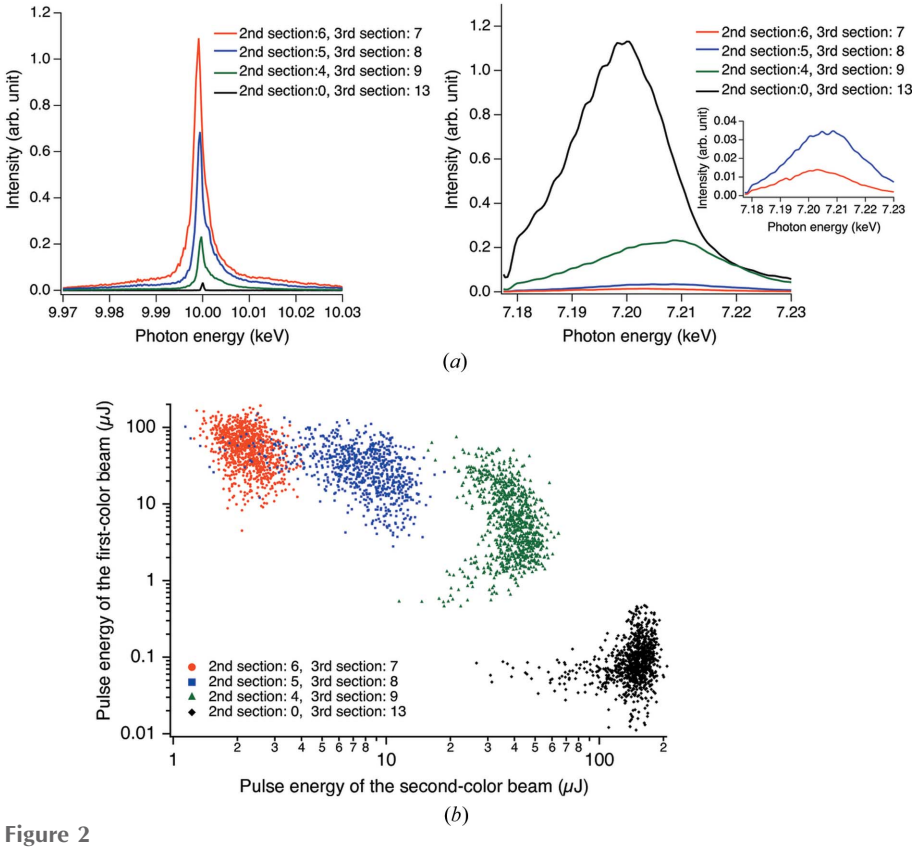

Figure 2
(*a*) Average spectra of the first-color (left) and the second-color (right) beams for different numbers of undulators in the second and the third sections. The inset of the right figure is the magnified spectra of the second-color beam for the number of undulators in the third section being seven and eight. (*b*) Shot-to-shot pulse energy correlation between the first-color and second-color beams.

4. Summary

In this paper, a new split-undulator scheme is proposed to generate a two-color XFEL consisting of broadband and narrowband beams. It has been experimentally confirmed that a two-color XFEL beam with a photon energy separation of ∼30% can be generated at

SACLA. Furthermore, it was also demonstrated that the intensity ratio between the first-color and second-color beams was controllable over a wide range. This unique two-color XFEL beam will expand the potential of XFELs for investigating interactions between intense X-rays and matter.

Acknowledgements

The authors acknowledge Dr K. Tamasaku, Dr E. E. McBride, Professor J. B. Hastings and Professor U. Bergmann for motivating this research.

Funding information

This study was supported by JSPS KAKENHI (grant No. 19K20604) and partially performed with the approval of the Japan Synchrotron Radiation Research Institute (proposal Nos. 2018A8040, 2018B8023 and 2019A8021).

References

Decking, W. *et al.* (2020). *Nat. Photon.* **14**, 391–397.

Emma, P., Akre, R., Arthur, J., Bionta, R., Bostedt, C., Bozek, J., Brachmann, A., Bucksbaum, P., Coffee, R., Decker, F., Ding, Y., Dowell, D., Edstrom, S., Fisher, A., Frisch, J., Gilevich, S., Hastings, J., Hays, G., Hering, P., Huang, Z., Iverson, R., Loos, H., Messerschmidt, M., Miahnahri, A., Moeller, S., Nuhn, H., Pile, G., Ratner, D., Rzepiela, J., Schultz, D., Smith, T., Stefan, P., Tompkins, H., Turner, J., Welch, J., White, W., Wu, J., Yocky, G. & Galayda, J. (2010). *Nat. Photon.* **4**, 641–647.

Ghimire, S., Fuchs, M., Hastings, J., Herrmann, S. C., Inubushi, Y., Pines, J., Shwartz, S., Yabashi, M. & Reis, D. A. (2016). *Phys. Rev. A*, **94**, 043418.

Glenzer, S. H. & Redmer, R. (2009). *Rev. Mod. Phys.* **81**, 1625–1663.

Glover, T. E., Fritz, D. M., Cammarata, M., Allison, T. K., Coh, S., Feldkamp, J. M., Lemke, H., Zhu, D., Feng, Y., Coffee, R. N., Fuchs, M., Ghimire, S., Chen, J., Shwartz, S., Reis, D. A., Harris, S. E. & Hastings, J. B. (2012). *Nature*, **488**, 603–608.

Gorel, A., Motomura, K., Fukuzawa, H., Doak, R. B., Grünbein, M. L., Hilpert, M., Inoue, I., Kloos, M., Kovácsová, G., Nango, E., Nass, K., Roome, C. M., Shoeman, R. L., Tanaka, R., Tono, K., Joti, Y., Yabashi, M., Iwata, S., Foucar, L., Ueda, K., Barends, T. R. M. & Schlichting, I. (2017). *Nat. Commun.* **8**, 1170.

Hara, T., Inubushi, Y., Katayama, T., Sato, T., Tanaka, H., Tanaka, T., Togashi, T., Togawa, K., Tono, K., Yabashi, M. & Ishikawa, T. (2013). *Nat. Commun.* **4**, 2919.

Inoue, I., Hara, T., Inubushi, Y., Tono, K., Inagaki, T., Katayama, T., Amemiya, Y., Tanaka, H. & Yabashi, M. (2018). *Phys. Rev. Accel. Beams*, **21**, 080704.

Inoue, I., Inubushi, Y., Sato, T., Tono, K., Katayama, T., Kameshima, T., Ogawa, K., Togashi, T., Owada, S., Amemiya, Y., Tanaka, T., Hara, T. & Yabashi, M. (2016). *Proc. Natl Acad. Sci. USA*, **113**, 1492–1497.

Inoue, I., Osaka, T., Hara, T., Tanaka, T., Inagaki, T., Fukui, T., Goto, S., Inubushi, Y., Kimura, H., Kinjo, R., Ohashi, H., Togawa, K., Tono, K., Yamaga, M., Tanaka, H., Ishikawa, T. & Yabashi, M. (2019). *Nat. Photon.* **13**, 319–322.

Inubushi, Y., Inoue, I., Kim, J., Nishihara, A., Matsuyama, S., Yumoto, H., Koyama, T., Tono, K., Ohashi, H., Yamauchi, K. & Yabashi, M. (2017). *Appl. Sci.* **7**, 584.

Ishikawa, T., Aoyagi, H., Asaka, T., Asano, Y., Azumi, N., Bizen, T., Ego, H., Fukami, K., Fukui, T., Furukawa, Y., Goto, S., Hanaki, H., Hara, T., Hasegawa, T., Hatsui, T., Higashiya, A., Hirono, T., Hosoda, N., Ishii, M., Inagaki, T., Inubushi, Y., Itoga, T., Joti, Y., Kago, M., Kameshima, T., Kimura, H., Kirihara, Y., Kiyomichi, A., Kobayashi, T., Kondo, C., Kudo, T., Maesaka, H., Maréchal, X. M., Masuda, T., Matsubara, S., Matsumoto, T., Matsushita, T., Matsui, S., Nagasono, M., Nariyama, N., Ohashi, H., Ohata, T., Ohshima, T., Ono, S., Otake, Y., Saji, C., Sakurai, T., Sato, T., Sawada, K., Seike, T., Shirasawa, K., Sugimoto, T., Suzuki, S., Takahashi, S., Takebe, H., Takeshita, K., Tamasaku, K., Tanaka, H., Tanaka, R., Tanaka, T., Togashi, T., Togawa, K., Tokuhisa, A., Tomizawa, H., Tono, K., Wu, S., Yabashi, M., Yamaga, M., Yamashita, A., Yanagida, K., Zhang, C., Shintake, T., Kitamura, H. & Kumagai, N. (2012). *Nat. Photon.* **6**, 540–544.

Kameshima, T., Ono, S., Kudo, T., Ozaki, K., Kirihara, Y., Kobayashi, K., Inubushi, Y., Yabashi, M., Horigome, T., Holland, A., Holland, K., Burt, D., Murao, H. & Hatsui, T. (2014). *Rev. Sci. Instrum.* **85**, 033110.

Kang, H. S., Min, C., Heo, H., Kim, C., Yang, H., Kim, G., Nam, I., Baek, S. Y., Choi, H., Mun, G., Park, B. R., Suh, Y. J., Shin, D. C., Hu, J., Hong, J., Jung, S., Kim, S., Kim, K., Na, D., Park, S. S., Park, Y. J., Han, J., Jung, Y. G., Jeong, S. H., Lee, H. G., Lee, S., Lee, S., Lee, W., Oh, B., Suh, H. S., Parc, Y. W., Park, S., Kim, M. H., Jung, N., Kim, Y., Lee, M., Lee, B., Sung, C., Mok, I., Yang, J., Lee, C., Shin, H., Kim, J. H., Kim, Y., Lee, J. H., Park, S., Kim, J., Park, J., Eom, I., Rah, S., Kim, S., Nam, K. H., Park, J., Park, J., Kim, S., Kwon, S., Park, S. H., Kim, K. S., Hyun, H., Kim, S. N., Kim, S., Hwang, S., Kim, M. J., Lim, C., Yu, C., Kim, B., Kang, T., Kim, K., Kim, S., Lee, H., Lee, H., Park, K., Koo, T., Kim, D. & Ko, I. S. (2017). *Nat. Photon.* **11**, 708–713.

Katayama, T., Owada, S., Togashi, T., Ogawa, K., Karvinen, P., Vartiainen, I., Eronen, A., David, C., Sato, T., Nakajima, K., Joti, Y., Yumoto, H., Ohashi, H. & Yabashi, M. (2016). *Struct. Dyn.* **3**, 034301.

McNeil, B. W. J. & Thompson, N. R. (2010). *Nat. Photon.* **4**, 814–821.

Milne, C. J., Schietinger, T., Aiba, M., Alarcon, A., Alex, J., Anghel, A., Arsov, V., Beard, C., Beaud, P., Bettoni, S., Bopp, M., Brands, H., Brönnimann, M., Brunnenkant, I., Calvi, M., Citterio, A., Craievich, P., Csatari Divall, M., Dällenbach, M., D'Amico, M., Dax, A., Deng, Y., Dietrich, A., Dinapoli, R., Divall, E., Dordevic, S., Ebner, S., Erny, C., Fitze, H., Flechsig, U., Follath, R., Frei, F., Gärtner, F., Ganter, R., Garvey, T., Geng, Z., Gorgisyan, I., Gough, C., Hauff, A., Hauri, C., Hiller, N., Humar, T., Hunziker, S., Ingold, G., Ischebeck, R., Janousch, M., Juranić, P., Jurcevic, M., Kaiser, M., Kalantari, B., Kalt, R., Keil, B., Kittel, C., Knopp, G., Koprek, W., Lemke, H., Lippuner, T., Llorente Sancho, D., Löhl, F., Lopez-Cuenca, C., Märki, F., Marcellini, F., Marinkovic, G., Martiel, I., Menzel, R., Mozzanica, A., Nass, K., Orlandi, G., Ozkan Loch, C., Panepucci, E., Paraliev, M., Patterson, B., Pedrini, B., Pedrozzi, M., Pollet, P., Pradervand, C., Prat, E., Radi, P., Raguin, J., Redford, S., Rehanek, J., Réhault, J., Reiche, S., Ringele, M., Rittmann, J., Rivkin, L., Romann, A., Ruat, M., Ruder, C., Sala, L., Schebacher, L., Schilcher, T., Schlott, V., Schmidt, T., Schmitt, B., Shi, X., Stadler, M., Stingelin, L., Sturzenegger, W., Szlachetko, J., Thattil, D., Treyer, D., Trisorio, A., Tron, W., Vetter, S., Vicario, C., Voulot, D., Wang, M., Zamofing, T., Zellweger, C., Zennaro, R., Zimoch, E., Abela, R., Patthey, L. & Braun, H. (2017). *Appl. Sci.* **7**, 720.

Mimura, H., Yumoto, H., Matsuyama, S., Koyama, T., Tono, K., Inubushi, Y., Togashi, T., Sato, T., Kim, J., Fukui, R., Sano, Y., Yabashi, M., Ohashi, H., Ishikawa, T. & Yamauchi, K. (2014). *Nat. Commun.* **5**, 3539.

Osaka, T., Inoue, I., Kinjo, R., Hirano, T., Morioka, Y., Sano, Y., Yamauchi, K. & Yabashi, M. (2019). *J. Synchrotron Rad.* **26**, 1496–1502.

Shwartz, S., Fuchs, M., Hastings, J., Inubushi, Y., Ishikawa, T., Katayama, T., Reis, D., Sato, T., Tono, K., Yabashi, M., Yudovich, S. & Harris, S. (2014). *Phys. Rev. Lett.* **112**, 163901.

Tamasaku, K., Shigemasa, E., Inubushi, Y., Inoue, I., Osaka, T., Katayama, T., Yabashi, M., Koide, A., Yokoyama, T. & Ishikawa, T. (2018). *Phys. Rev. Lett.* **121**, 083901.

Tamasaku, K., Shigemasa, E., Inubushi, Y., Katayama, T., Sawada, K., Yumoto, H., Ohashi, H., Mimura, H., Yabashi, M., Yamauchi, K. & Ishikawa, T. (2014). *Nat. Photon.* **8**, 313–316.
Tono, K., Kudo, T., Yabashi, M., Tachibana, T., Feng, Y., Fritz, D., Hastings, J. & Ishikawa, T. (2011). *Rev. Sci. Instrum.* **82**, 023108.
Tono, K., Togashi, T., Inubushi, Y., Sato, T., Katayama, T., Ogawa, K., Ohashi, H., Kimura, H., Takahashi, S., Takeshita, K., Tomizawa, H., Goto, S., Ishikawa, T. & Yabashi, M. (2013). *New J. Phys.* **15**, 083035.
Vinko, S. M., Ciricosta, O., Cho, B. I., Engelhorn, K., Chung, H., Brown, C. R. D., Burian, T., Chalupský, J., Falcone, R. W., Graves, C., Hájková, V., Higginbotham, A., Juha, L., Krzywinski, J., Lee, H. J., Messerschmidt, M., Murphy, C. D., Ping, Y., Scherz, A., Schlotter, W., Toleikis, S., Turner, J. J., Vysin, L., Wang, T., Wu, B., Zastrau, U., Zhu, D., Lee, R. W., Heimann, P. A., Nagler, B. & Wark, J. S. (2012). *Nature*, **482**, 59–62.
Xie, M. (2000). *Nucl. Instrum. Methods Phys. Res. A*, **445**, 59–66.
Yabashi, M., Tanaka, H. & Ishikawa, T. (2015). *J. Synchrotron Rad.* **22**, 477–484.
Yoneda, H., Inubushi, Y., Nagamine, K., Michine, Y., Ohashi, H., Yumoto, H., Yamauchi, K., Mimura, H., Kitamura, H., Katayama, T., Ishikawa, T. & Yabashi, M. (2015). *Nature*, **524**, 446–449.
Yumoto, H., Inubushi, Y., Osaka, T., Inoue, I., Koyama, T., Tono, K., Yabashi, M. & Ohashi, H. (2020). *Appl. Sci.* **10**, 2611.